



# Effects of modified biochar on water and salt distribution and water-stable macro-aggregates in saline-alkaline soil

Manli Duan<sup>1</sup> · Guohuan Liu<sup>1</sup> · Beibei Zhou<sup>1</sup> · Xiaopeng Chen<sup>1</sup> · Quanjiu Wang<sup>1</sup> · Hongyan Zhu<sup>1</sup> · Zhijian Li<sup>1</sup>

Received: 12 August 2020 / Accepted: 24 February 2021 / Published online: 11 March 2021

© The Author(s), under exclusive licence to Springer-Verlag GmbH Germany, part of Springer Nature 2021

## Abstract

**Purpose** This study investigated the chemical and physical mechanisms associated with the movement of water and salt in saline-alkali soil amended with different types of biochar.

**Materials and methods** Four types of biochar were selected: ordinary laboratory-prepared biochar (BC), acidified biochar (HBC), particle size modified biochar (NBC), and composite modified biochar (HNBC). The physical and chemical properties of the biochar treatments were characterized. Vertical infiltration simulation tests were conducted to analyze the effects of modification on the adsorption and distribution of salt ions on biochar, and the soil water-stable macro-aggregates in saline-alkali soil.

**Results and discussion** The porous structure, specific surface area (SSA), micropore volume (VMIC), and H/C value were increased by acidification, particle size modification, and composite modification. Compared with BC, HBC and HNBC enhanced the O/C and (O+N)/C values, thereby increasing the hydrophilicity. The vertical infiltration tests showed that the depth of the soil wetting peak and cumulative infiltration were both higher than in the control (CK) after adding biochar, where HBC had the greatest water retention capacity. The modified biochar reduced the salt content and water-soluble Na<sup>+</sup> content of the soil profile by increasing the soil water content and adsorbing Na<sup>+</sup>. The modified biochar promoted the formation and stabilization of soil water-stable macro-aggregates. Amending soil with HBC showed the greatest reduction in salt content and increased water-stable macro-aggregation.

**Conclusions** HBC improved the water retention and Na<sup>+</sup> adsorption capacity of biochar. This enhanced the formation of soil water-stable macro-aggregates and improved the effects of biochar on saline-alkali soil by altering soil physical and chemical properties.

**Keywords** Modified biochar · Saline-alkaline soil · Sodium ion · Soil water-stable macro-aggregate · Water and salt transport

## 1 Introduction

Soil salinization negatively impacts agricultural production throughout the world, and its impact is increasing (Ivushkin et al. 2019). The base ion contents of saline-alkali soils are excessively high, which hinders crop growth and causes damage, thereby reducing yields and constraining agricultural

development. It is important to improve conditions for crop growth in saline-alkali land to ensure global food security.

Biochar can be useful for soil remediation. Biochar is formed by heating biological materials under anoxic or anaerobic conditions, which creates a black solid product with high aromatization that is resistant to decomposition (Mao et al. 2019). Biochar has an irregular pore structure, high specific surface area (SSA), and rough surface, and it is rich in carbon- and oxygen-containing functional groups, e.g., hydroxyl, carboxyl, and carbonyl groups (Mahdi et al. 2019). Previous studies have shown that adding biochar to soil can reduce the soil bulk density, improve the soil structure, and increase the water infiltration rate and saturated hydraulic conductivity (Obia et al. 2016; Zhao et al. 2019). Günel et al. (2018) demonstrated that biochar can significantly increase the soil

---

Responsible editor: Hailong Wang

✉ Beibei Zhou  
378179340@qq.com

<sup>1</sup> State Key Laboratory of Eco-hydraulics in Northwest Arid Region of China, Xi'an University of Technology, Xi'an 710048, China

porosity, available water content, and field capacity and reduce the soil wilting coefficient. Biochar can dilute the soil solution and alleviate salt stress by improving the water-holding capacity (Yue et al. 2016). Biochar has a strong capacity for adsorbing salts on its surface or in pores, thereby reducing salt concentrations in the soil solution (Akhtar et al. 2015; Hammer et al. 2015). Moreover, biochar can increase the soil organic carbon and nutrient contents, especially  $K^+$ ,  $Ca^{2+}$ ,  $Mg^{2+}$ ,  $Zn^{2+}$ , and  $Mn^{2+}$ . The increased availability of  $Ca^{2+}$  and  $Mg^{2+}$  can replace  $Na^+$  in soil (Usman et al. 2016; Yue et al. 2016; Zheng et al. 2018a) which contributes to improved aggregation and the quality of saline-alkali soil (Chaganti and Crohn 2015).

Biochar is weakly alkaline and contains high amounts of mineral salts. Thus, if a large amount of alkaline biochar is applied to saline-alkali land, the degree of soil salinization will be exacerbated (Blok et al. 2017; Luo et al. 2017; Zheng et al. 2018a). Altering the structure and properties of biochar can help address the problems associated with the application of alkaline biochar to saline-alkali soil and improve the effects of biochar on the soil moisture and salinity. For example, Mahdi et al. (2019) applied  $H_3PO_4$ ,  $H_2SO_4$ ,  $HNO_3$ ,  $HCl$ , and other strong acids to biochar and modified the properties. They found that acidification of biochar removed impurities such as metals, and acid functional groups were introduced onto the biochar surface to improve its porous structure. Vithanage et al. (2015) found that acidification increased the number and composition of the oxygen-containing functional groups on the surface of biochar, increased the SSA, and changed the surface structure characteristics to reduce the loss of soil water and nutrients. Kumari et al. (2016) showed that acid biochar with a lower pH might reduce the net negative surface charge, thereby resulting in soil flocculation and significantly improving hydraulic conductivity compared with alkaline biochar. In addition, the size of biochar particles affects the soil hydrological properties, and it has complex interactions with the saturated hydraulic conductivity of the soil and the large aggregate contents (Lu et al. 2019; Gamage et al. 2016). The SSA is larger when the biochar particle size is smaller (Xie et al. 2015), which could increase the amount of active sorption sites (Li et al. 2020) and increase the adsorption capacity for inorganic ions (Mahmoud et al. 2020). Nano-biochar contains more oxygen-containing functional groups (Li et al. 2020) and fatty chains and exhibits high dynamic stability and reaction capacities (Song et al. 2019), which could increase anion adsorption capacity by interacting with anions (Mahmoud et al. 2020). Therefore, we hypothesize that amending soil with modified biochar will increase soil hydraulic conductivity and decrease salinity compared to soil amended with ordinary biochar and that this will be attributed to the properties of the modified biochar. In addition, the stability of soil aggregates is an important factor that affects the movement and distribution of soil water and salt. Thus, it is

important to study the relationships between soil aggregates, soil moisture, and salinity after adding biochar.

In this study, apple branches with high lignin contents were used as raw materials to prepare biochar. Compared with crop straw biochar, apple branch biochar has a lower ash content, higher SSA, and higher carbon content (Yang et al. 2020; Tan et al. 2019), as well as a greater adsorption capacity. The apple tree biochar was acidified, decreased to nanometer particle size, and characterized. The aims of this study were (1) to analyze the effects of adding different types of modified biochar on the movement and distribution of soil water and salt and (2) to explore the mechanism responsible for the effects of modified biochar on the relationships between soil water-stable large aggregates and the distributions of soil water and salt.

## 2 Materials and methods

### 2.1 Experimental soil

The experimental soil was collected from the Lubotan area of Fuping County, Shaanxi Province, China (N 34°74', E 109°16'), where the average annual precipitation is 484 mm and the annual evaporation is 1000–1300 mm (Fig. 1). The thickness of the aquifer was about 10 m, with poor water permeability and low water richness. The groundwater depth was about 1 m, and the soil salt content averaged 0.596%, ranging from 0.09–1.91%. Soil was collected from the 0–20 cm layer from a local farm. The soil was air-dried, milled, and screened through a 2-mm mesh. The solid particle size composition is determined by laser particle size analyzer (Mastersizer 2000, UK) laser particle size analyzer. The volume fractions of clay, silt, and sand were 2.01%, 17.54%, and 80.44%, respectively. According to the international soil texture classification standard, the soil texture was sandy loam. The basic physical and chemical properties of the soil were as follows: pH, 8.3; bulk density, 1.45 g/cm<sup>3</sup>; initial water content, 2.87%; and salt content, 5.56 g/kg, and thus, it was characterized as a moderate saline-alkaline soil. The  $Na^+$ ,  $K^+$ ,  $Ca^{2+}$ , and  $Mg^{2+}$  contents were 0.597, 0.112, 0.057, and 0.064 g/kg, respectively.

### 2.2 Pretreatment of modified biochar

The apple tree branches were cut into 2 cm sections and carbonized in a carbonization furnace at 500°C for 3 h. Next, BC with a particle size of 1 mm was obtained by passing through a coarse crusher. NBC with a particle size of 10 nm was obtained by grinding BC to a particle size of 1 mm using a nano-grinding machine. BC and NBC were mixed with 20% (wt.)  $H_2SO_4$  solutions at an impregnation weight ratio of 1:20 at a constant temperature of 70°C for 6 h to create the modified biochar treatments. The modified biochars (HBC and HNBC)

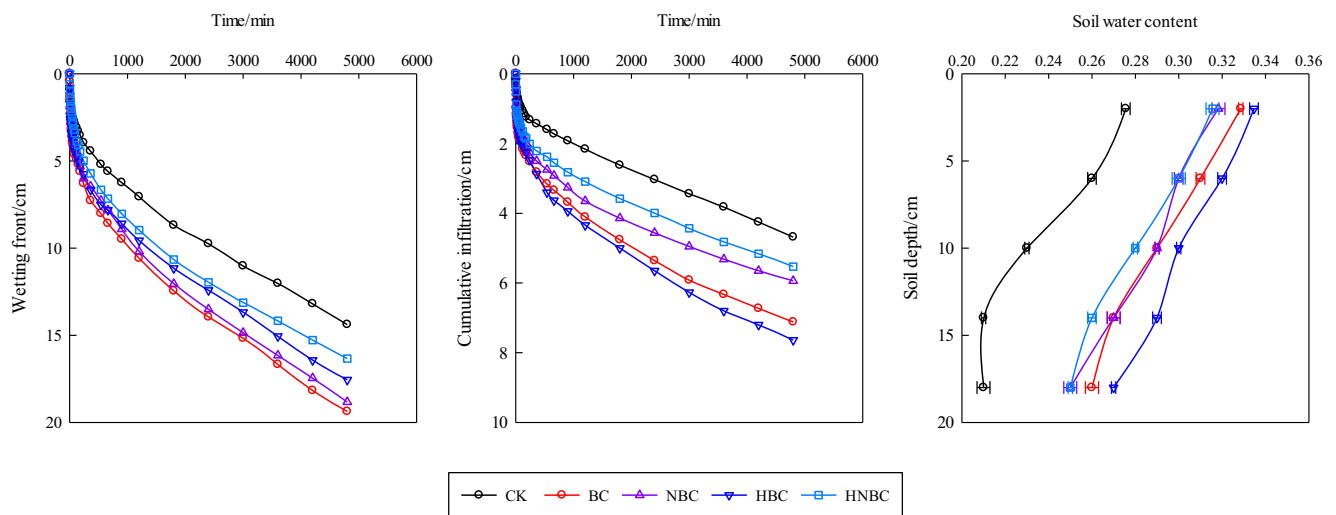


**Fig. 1** Infiltration characteristics of soil after adding biochar and modified biochar treatments

were washed with distilled water until the pH was constant and then dried at 70°C. The four types of biochar were placed in sealed bags and stored in desiccators until use.

### 2.3 Experimental design

Soil was mixed with each type of biochar (BC, NBC, HBC, and HNBC) at a rate of 1.0% (w/w) (Li and Shangguan 2018). A control treatment (CK) without added biochar was included. The soil-biochar mixtures were used to fill plexiglass columns with a diameter of 9 cm and height of 40 cm. The soil bulk density after filling was 1.45 g/cm<sup>3</sup>. To ensure a uniform soil column, the columns were packed in 5 cm increments to a height of 30 cm. Water was supplied to the soil at a constant pressure with a head height of 2 cm using a plexiglass bottle. When the soil wetting front reached 20 cm from the surface, the water application was stopped, and layered sampling started after the surface water was absorbed. The sampling depths were 2, 6, 10, 14, and 18 cm. An illustration of the experimental equipment is shown in Fig. S2. During the test, the soil wetting peak in the soil column and water level in the constant pressure bottle were recorded. Five treatments were tested in the experiment, with three replicates for each treatment.

### 2.4 Determination of chemical and physical properties

The elemental contents (C, N, O, and H) of the biochar were determined using an elemental analyzer (MICRO, Elementar, Germany). The pH of the biochar was determined using a pH meter (Mettler Toledo, Switzerland; sample: water ratio of 1:2.5 w/v). SSA was determined for the biochar using a specific surface area and pore size analyzer (V-Sorb 2800TP, Gold APP instruments Corp., China). A field emission scanning electron microscope

was used to observe the surface morphology of the four types of biochar. The cation exchange capacity (CEC) of the biochar was determined with the BaCl<sub>2</sub>–H<sub>2</sub>SO<sub>4</sub> method. The soil water content was determined using the drying method (105 ± 2°C). The soil electrical conductivity (EC) was measured with a conductivity meter (DDS-307, Rex Electric Chemical, China; soil/water ratio of 1:5 w/v), and the soil EC was converted into the soil salt content using the mass method (residue drying). The water-soluble potassium and sodium ion contents of the soil samples were determined by flame photometry. The water-soluble calcium and magnesium ion contents of the soil samples were determined by atomic absorption spectrometry. The soil water-stable macro-aggregate contents were determined with a wet sieving device (Eijkelkamp Soil & Water, Netherlands), where 4.0 g of air-dried soil sample (1–2 mm particle size) was placed in a sieve with a pore size of 0.25 mm and washed with 100 mL of distilled water for 3 min and then with 100 mL of dispersion solution (for soil pH > 7, 2 g sodium hexametaphosphate per 1 L) for 8 min. The soil water-stable macro-aggregate content was equal to the soil weight obtained in the dispersing solution divided by the sum of the soil weight obtained in the dispersing solution and distilled water.

### 2.5 Infiltration model

The Philip model (Philip 1957), Kostiakov model (Kostiakov 1932), and Horton model (Horton 1933) were used to analyze the effects of the modified biochar samples on the parameters of the soil infiltration formulas. This was done to assess the influence of the modified biochar samples on the water infiltration characteristics.

1) Philip model:

$$i(t) = \frac{1}{2}St^{-0.5} + A,$$

where  $i(t)$  is the soil infiltration rate, cm/min;  $t$  is the infiltration duration, min;  $S$  is the imbibition rate, cm/min<sup>1/2</sup>; and  $A$  is the empirical coefficient.

2) Kostiakov model:

$$i(t) = at^{-b},$$

where  $a$  and  $b$  are the empirical coefficients.

3) Horton model:

$$i(t) = i_c + (i_0 - i_c)e^{-kt},$$

where  $i_0$  is the initial infiltration rate, cm/min;  $i_c$  is the stable infiltration rate, cm/min; and  $k$  is the empirical coefficient.

## 2.6 Data processing and analysis

Excel 2017 and SPSS 23.0 were used for basic statistical data analyses and to conduct Duncan’s multiple comparison tests ( $P < 0.05$ ), respectively. SigmaPlot 14.0 software was used for mapping.

## 3 Results and discussion

### 3.1 Physical and chemical properties of modified biochar samples

Table 1 shows that the C and H contents increased in the modified biochar samples, whereas the O content increased

significantly after acidification. The O/C values in HBC and HNBC were 2.21 and 2.58 times higher than in BC, respectively, and the (O+N)/C values in HBC and HNBC were 1.94 and 2.10 times higher than in BC, respectively. These results indicate that oxygen-containing functional groups were more abundant on the surface of HBC than BC, where they enhanced the hydrophilicity and polarity of the biochar (Wang et al. 2015). The H/C values for NBC, HBC, and HNBC were higher than those for BC, thereby indicating that the aromaticity of the modified biochar decreased, whereas the C stability increased (Hammes et al. 2006; Wang et al. 2020). The CEC values determined for the four types of biochar differed significantly ( $P < 0.05$ ). The CEC values for HBC and HNBC were 5.02% and 14.55% higher, respectively, compared with BC, and thus acidification and composite modification of the biochar were beneficial for improving the soil CEC (Xu et al. 2012). The pH values for HBC and HNBC decreased from 9.39 to 3.06 and 3.25, respectively. The pH values of the soils mixed with 1% HBC and HNBC reduced by 0.13 and 0.07 units, respectively, compared with BC, possibly because the higher CEC values for HBC and HNBC improved the pH buffering capacity of the soil (Amoah-Antwi et al. 2020).

The SSA and microporous volume (VMIC) of biochar were increased in the three modified treatments, and the increased SSA provided more sites for ion adsorption. Compared with BC, the SSA and VMIC were 2.36 and 1.95 times higher for HNBC, respectively. Scanning electron microscopy (SEM) clearly indicated that HBC and BC had porous structures (Fig. S3). NBC and HNBC lacked obvious porous structures even at 10,000 times magnification due to the small particle size and large pore structure. The increases in SSA and the porous structure of the biochar after acidification can be explained by the acid dissolving inorganic components of the biochar (Chang et al. 2019), leaching ash from the surface and pores, hydrolyzing or solubilizing organic matter, and exposing more micropores (Pongkua et al. 2020; Rizwan et al. 2020). Particle size modification degraded the biochar and changed the pore structure by increasing the numbers of cracks and fissures (Sangani et al. 2020) to expose inaccessible pores, thereby increasing the SSA and micropore rate in NBC and HNBC (Xie et al. 2015; Sun et al. 2012).

**Table 1** Physical and chemical properties of modified biochar samples

Biochar	C (%)	H (%)	O (%)	N (%)	O/C	(O+N)/C	H/C	SSA (m <sup>2</sup> /g)	VMIC (cm <sup>3</sup> /g)	CEC (cmol/kg)	pH (biochar)	pH (soil with 1.0% biochar)
BC	85.75	0.47	2.04	0.60	0.024	0.031	0.0055	195.3	0.084	259.1±3.2c	9.39±0.02b	8.22±0.03b
NBC	87.63	0.74	0.67	0.39	0.008	0.012	0.0084	407.5	0.150	247.9±2.9d	9.73±0.03a	8.30±0.02a
HBC	86.15	0.70	4.56	0.61	0.053	0.060	0.0081	248.4	0.113	272.1±1.1b	3.06±0.01d	8.09±0.01d
HNBC	91.98	1.33	5.68	0.32	0.062	0.065	0.0145	461.4	0.164	296.8±2.5a	3.25±0.04c	8.15±0.02c

Different letters in the same column indicate significant differences ( $P < 0.05$ )

## 3.2 Effects of biochar modifications on water movement

### 3.2.1 Effects of biochar modifications on water infiltration

The movement of salt in the soil is readily affected by the soil water content, and thus, it is important to study the infiltration of water into the soil in saline-alkali land. The changes in the soil wetting peak with the infiltration time after adding biochar are shown in Fig. 1a. For the same infiltration time, the migration distance of the soil wetting peak increased after adding biochar compared with CK. To reach the same wetting front migration distance, the required infiltration times with the modified types of biochar were longer compared with BC. At the end of infiltration, the times required for CK, BC, NBC, HBC, and HNBC were 8285, 5120, 5390, 6105, and 7090 min, respectively, which indicates that biochar improved the soil permeability and contributed to soil water infiltration. Amending soil with the modified biochar treatments reduced the rate of water movement in the soil compared with the unmodified biochar.

Cumulative infiltration over time for all treatments is shown in Fig. 1b. Compared with CK, cumulative infiltration was greater in soil amended with biochar at the same infiltration time, and HBC had the largest cumulative infiltration. At the end of infiltration, the cumulative soil infiltration volumes with CK, BC, NBC, HBC, and HNBC were 6.39, 7.33, 6.47, 8.70, and 6.96 cm, respectively, and the infiltration rates were 0.77, 1.43, 1.16, 1.47, and 0.98 cm/min, respectively. These results indicate that the addition of biochar increased the soil water infiltration rate, and acidification had the greatest effect on promoting the infiltration of water and increasing the amount of infiltration.

Changes to the soil water content after water addition under each treatment at various soil depths are shown in Fig. 1c. When the infiltrating water reached a depth of 20 cm, the soil water contents in the 0–4 cm soil layer under BC, NBC, HBC, and HNBC increased by 19.26%, 15.52%, 21.45%, and 14.51%, respectively, compared with CK. These results demonstrate that the addition of biochar increased the soil permeability and water conductivity, and improved the soil water-holding capacity and water retention. Similar results were obtained by Zong et al. (2015). In particular, HBC had the highest cumulative soil infiltration rate and moisture content throughout the soil profile, and thus it had the greatest effect on increasing the retention of water in saline-alkali soil.

Biochar may have improved the soil water-holding capacity for a few reasons. Firstly, biochar has a high potential for  $\text{Na}^+$  adsorption, thereby alleviating the swelling

and dispersion of clay due to the high  $\text{Na}^+$  content of the soil. This would increase the soil permeability and hydraulic conductivity (Amini et al. 2015). Secondly, biochar can improve the physical structure of soil by reducing the bulk density (Zhao et al. 2019), increasing the porosity, and improving aggregate stability. This would help increase the infiltration rate and soil infiltration capacity (Ahmadi et al. 2020). Thirdly, the effect of biochar modification on soil water retention was related to the modification method. After acidification, the biochar had an obvious porous structure. This enhanced the hydrophilicity and polarity and facilitated soil moisture storage. Compared with acidification, particle size modification reduced the oxygen-containing functional groups on the biochar to decrease the hydrophilicity and polarity. In addition, the particle size was reduced to the nano-scale and the original macroporous structure of the biochar was destroyed, thereby allowing water to pass through more readily, blocking the soil micropores (Zhao et al. 2019), and reducing the soil permeability.

### 3.2.2 Effects of biochar modifications on soil infiltration parameters

The biochar modifications had differing effects on the soil infiltration characteristics. The Philip, Kostiakov, and Horton models were used to fit the soil water infiltration curves (Table 2). The coefficient of determination ( $R^2$ ) values ranged from 0.95 to 0.99 for the Philip model, 0.96 to 1.00 for the Kostiakov model, and 0.88 to 0.97 for the Horton model. All three models fitted the soil water infiltration curves well after adding the modified biochar treatments, and the Kostiakov model obtained the best fit. The infiltration rate  $S$  and empirical coefficient  $a$  reflect the soil infiltration rate and initial infiltration rate, respectively, and these values followed the order of  $\text{NBC} > \text{BC} > \text{HNBC} > \text{HBC}$ . These results indicate that the addition of biochar could increase the soil infiltration rate, but HBC and HNBC reduced this effect. The parameter  $b$  denotes the degree of attenuation of the infiltration rate. The  $b$  value was lower for BC than CK and was lower for HBC than BC. Thus, attenuation of the infiltration rate was slowest under HBC. In the Horton model, the initial infiltration rate  $i_0$  was higher for BC, NBC, and HNBC than CK, but the  $i_0$  value was lower for HBC than CK. These findings differed from the response of the empirical coefficient  $a$  in the Kostiakov model. This might be attributed to the poor fit of the Horton model for HBC. In summary, the infiltration rate  $S$  and parameters  $a$  and  $b$  reflected the increases in the soil infiltration rate after the addition of biochar, and acidified biochar reduced the attenuation of the soil infiltration rate.

**Table 2** Fitted results for infiltration formula parameters

Treatment	Philip model			Kostiakov model			Horton model			
	Imbibition rate ( <i>S</i> )	Empirical coefficient ( <i>A</i> )	<i>R</i> <sup>2</sup>	Empirical coefficient ( <i>a</i> )	Empirical coefficient ( <i>b</i> )	<i>R</i> <sup>2</sup>	Initial infiltration rate ( <i>i</i> <sub>0</sub> )	Stable infiltration rate ( <i>i</i> <sub>c</sub> )	Empirical coefficient ( <i>k</i> )	<i>R</i> <sup>2</sup>
CK	0.291	−0.004	0.987	0.149	0.594	0.996	0.176	0.009	0.209	0.911
BC	0.660	−0.006	0.966	0.318	0.509	0.961	0.311	0.012	0.089	0.969
NBC	0.749	−0.018	0.953	0.397	0.724	0.997	0.532	0.017	0.307	0.951
HBC	0.420	0.001	0.972	0.203	0.455	0.979	0.170	0.010	0.058	0.886
HNBC	0.594	−0.010	0.988	0.300	0.599	0.994	0.325	0.014	0.159	0.910

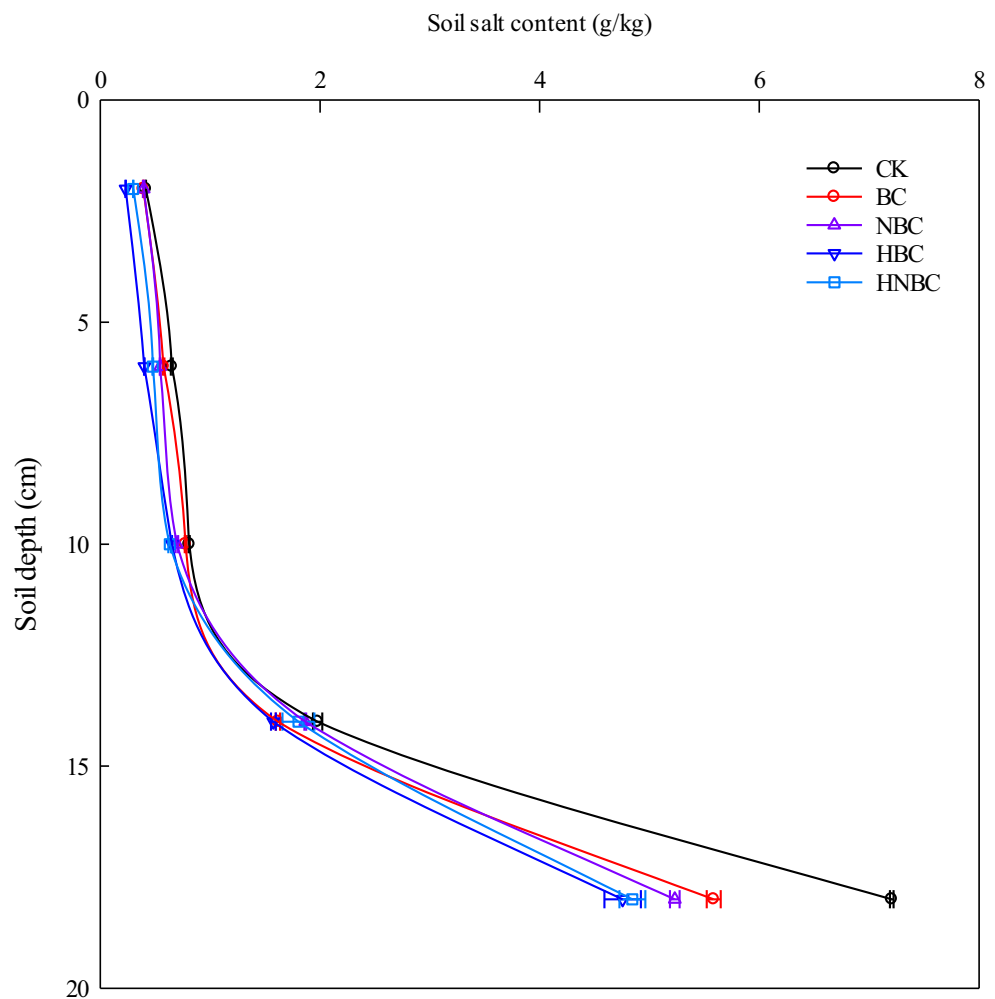
### 3.3 Effects of biochar modifications on salt distribution

#### 3.3.1 Effects of biochar modifications on distribution of the soil salt content

Figure 2 shows the salt content in the soil profile at the end of infiltration. The salt content of the soil included soluble salt.

The salt moved with the water, so the soil salt content gradually increased as the soil depth and water content increased. After adding biochar, the salinity of the soil profile decreased for all biochar treatments significantly compared with CK, where the reductions were between 4.11 and 44.53%, and the differences between the biochar treatments and the CK treatment were significant in the 12–16 cm and 16–20 cm soil layers (*P* < 0.05). Compared with BC, the salt content was

**Fig. 2** Distribution of salt content in different soil layers after adding biochar and modified biochar treatments



reduced further by the biochar modifications, where HBC had the lowest content. The results showed that the biochar modifications were more effective than BC at reducing the soil salt stress, and HBC had the greatest effect. This is because biochar has a strong adsorption capacity, and salt is adsorbed on the biochar surface or in the pores to reduce the salt content in the soil solution (Akhtar et al. 2015; Hammer et al. 2015). The biochar modifications were more effective than BC at reducing the soil salt content because the SSA of the biochar increased after acidification, particle size modification, and both modifications, and thus the contact area was larger with more adsorption sites and the maximum adsorption capacity increased (Zhu et al. 2018). Li et al. (2016) showed that the adsorption capacity of biochar is affected by the pH, where the competition for hydroxyl ions on the biochar surface at a higher pH reduces the adsorption capacity. In addition, acidification increased the abundance and diversity of oxygen-containing functional groups on biochar to improve the adsorption capacity (Chang et al. 2019), and thus HNBC was most effective at adsorption.

### 3.3.2 Effects of biochar modifications on the distributions of water-soluble $\text{Na}^+$ , $\text{K}^+$ , $\text{Ca}^{2+}$ , and $\text{Mg}^{2+}$ in soil

Figure 3 a–d show the distributions of the water-soluble  $\text{Na}^+$ ,  $\text{K}^+$ ,  $\text{Ca}^{2+}$ , and  $\text{Mg}^{2+}$  contents in different soil layers

at the end of infiltration. Compared with CK, the biochar treatments had decreased water-soluble  $\text{Na}^+$  content throughout the whole soil profile, whereas the water-soluble  $\text{K}^+$  content increased in the 0–12 cm soil layer and decreased in the 12–20 cm lower soil layer. The water-soluble  $\text{Ca}^{2+}$  and  $\text{Mg}^{2+}$  contents increased throughout the soil profile, as also found by Huang et al. (2019). Biochar can release  $\text{K}^+$ ,  $\text{Ca}^{2+}$ ,  $\text{Mg}^{2+}$ , and other mineral nutrients into the soil (Amini et al. 2015; Ahmad et al. 2016), which are then adsorbed on soil colloids (Yue et al. 2016), and thus the  $\text{K}^+$ ,  $\text{Ca}^{2+}$ , and  $\text{Mg}^{2+}$  contents can be higher in soil with added biochar compared with those without biochar. In addition, the  $\text{K}^+$ ,  $\text{Ca}^{2+}$ , and  $\text{Mg}^{2+}$  released into the soil readily replaced  $\text{Na}^+$  at the exchange sites to reduce the water-soluble  $\text{Na}^+$  content of the soil, and similar results were reported by Xiao et al. (2020).

The biochar modifications had differing effects on the distributions of water-soluble  $\text{Na}^+$ ,  $\text{K}^+$ ,  $\text{Ca}^{2+}$ , and  $\text{Mg}^{2+}$ . In particular, the water-soluble  $\text{Na}^+$  content was lower in the whole soil profile with the HBC treatment compared to the other treatments, whereas the water-soluble  $\text{K}^+$ ,  $\text{Ca}^{2+}$ , and  $\text{Mg}^{2+}$  contents were higher in the HBC treatment compared with the other treatments. The water-soluble  $\text{Na}^+$  content with NBC differed from HBC. Thus, the adsorption of water-soluble  $\text{Na}^+$  by biochar was enhanced

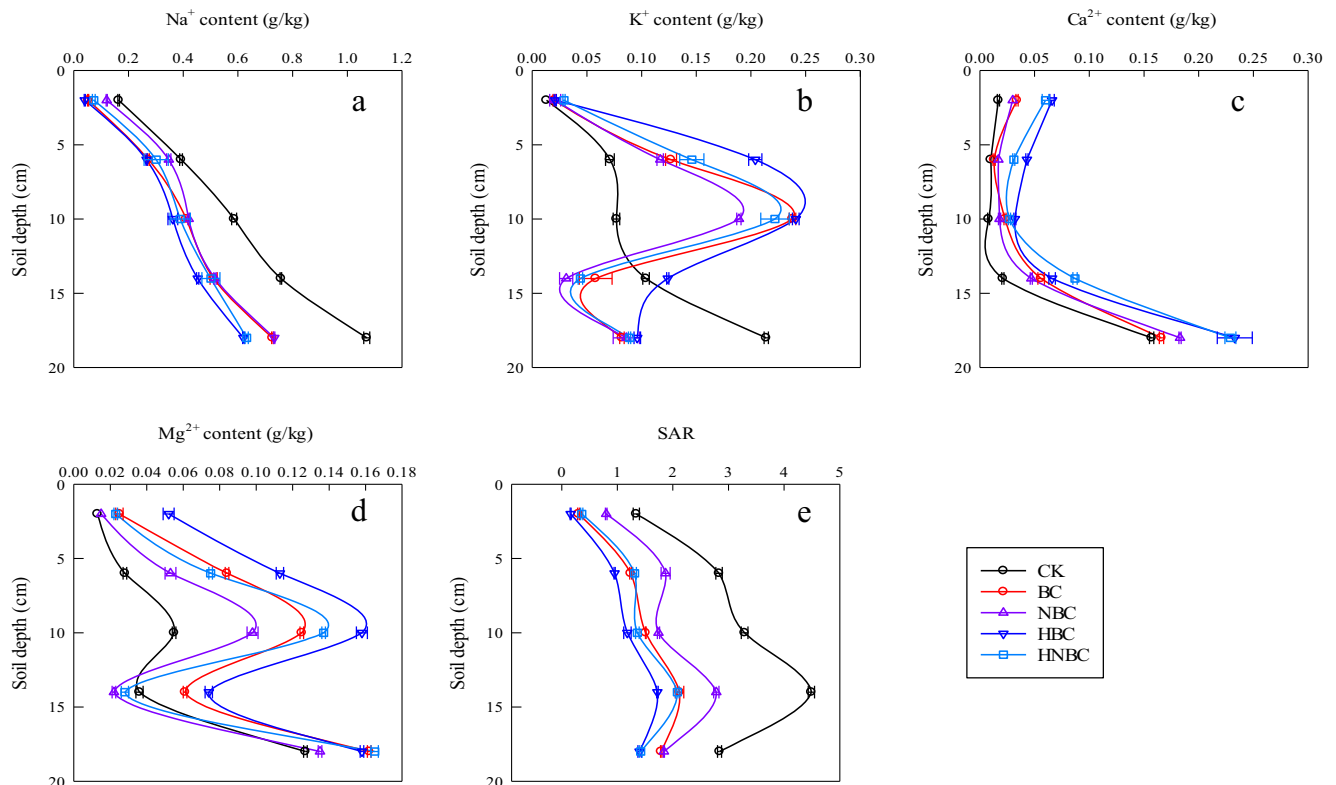


**Fig. 3** Distributions of soil soluble  $\text{Na}^+$ ,  $\text{K}^+$ ,  $\text{Ca}^{2+}$ , and  $\text{Mg}^{2+}$  and soil sodium adsorption ratio in the soil profile after adding biochar and modified biochar treatments

after acidification, which resulted in higher water-soluble  $K^+$ ,  $Ca^{2+}$ , and  $Mg^{2+}$  contents in the soil. The adsorption of  $Na^+$  was reduced after particle size modification, and the water-soluble  $K^+$ ,  $Ca^{2+}$ , and  $Mg^{2+}$  contents decreased. Acidification introduced acidic oxygen-containing functional groups ( $-COOH$ ,  $-OH$ , and  $-NO_2$ ) and increased the surface complexation of  $Na^+$  with carboxyl and hydroxyl functional groups (Chang et al. 2019). The potassium, calcium, and magnesium in the HBC were converted into an effective state, so the soil-soluble  $K^+$ ,  $Ca^{2+}$ , and  $Mg^{2+}$  contents increased.

The sodium adsorption ratio (SAR) is an important indicator for evaluating the degree of soil salinization. A higher SAR value indicates that the soil physical structure is more dispersed, and the water permeability is low. Figure 3e shows the changes in SAR in the soil profile after adding biochar. Adding the biochar treatments significantly reduced the SAR values in the different layers of the saline-alkali soil ( $P < 0.05$ ). The SAR values increased in order of  $HBC < HNBC < BC < NBC < CK$ . The SAR values were 64.24%, 58.79%, 54.02%, and 47.13% lower in NBC, BC, HNBC, and HBC, respectively, compared with CK in the 8–12 cm soil layer. Compared with NBC and HNBC, HBC significantly reduced the soil soluble  $Na^+$  and SAR but significantly increased the soil soluble  $K^+$ ,  $Ca^{2+}$ , and  $Mg^{2+}$  contents ( $P < 0.05$ ). Thus, HBC was most effective at reducing soil salinization.

### 3.4 Effects of biochar modifications on soil water-stable macro-aggregates

Soil water-stable macro-aggregates (particle size  $> 0.25$  mm) are important indicators for evaluating the physical quality of soil (Luo et al. 2018). Soil water-stable macro-aggregates do not disperse immediately after water immersion, and they ensure that the soil structure is retained under disturbances. Figure 4 shows the soil water-stable macro-aggregate contents in different soil layers at the end of infiltration. The plot of the soil water-stable macro-aggregate contents was S-shaped in the 0–20 cm soil layer, where the soil water-stable macro-aggregate content was highest from 8 to 12 cm, and the differences between the treatments were highly significant ( $P < 0.01$ ). Compared with CK, biochar increased the soil water-stable macro-aggregate contents in different soil layers, and similar results were obtained by Dong et al. (2016). Compared with BC, HBC, NBC, and HNBC all increased the soil water-stable aggregate contents. In the 0–15 cm soil layer, the aggregate content was highest with HBC, being 1.59–1.96 times and 1.45–1.80 times higher than in CK and BC, respectively. These results suggest that HBC effectively improved the soil water-stable macro-aggregate content.

Biochar can combine with soil particles by adsorbing to soil organic matter, coalescing many micro-aggregates into macro-aggregates, increasing the stability of soil aggregates,

**Fig. 4** Soil water-stable macro-aggregate contents in different soil layers after adding biochar and modified biochar treatments

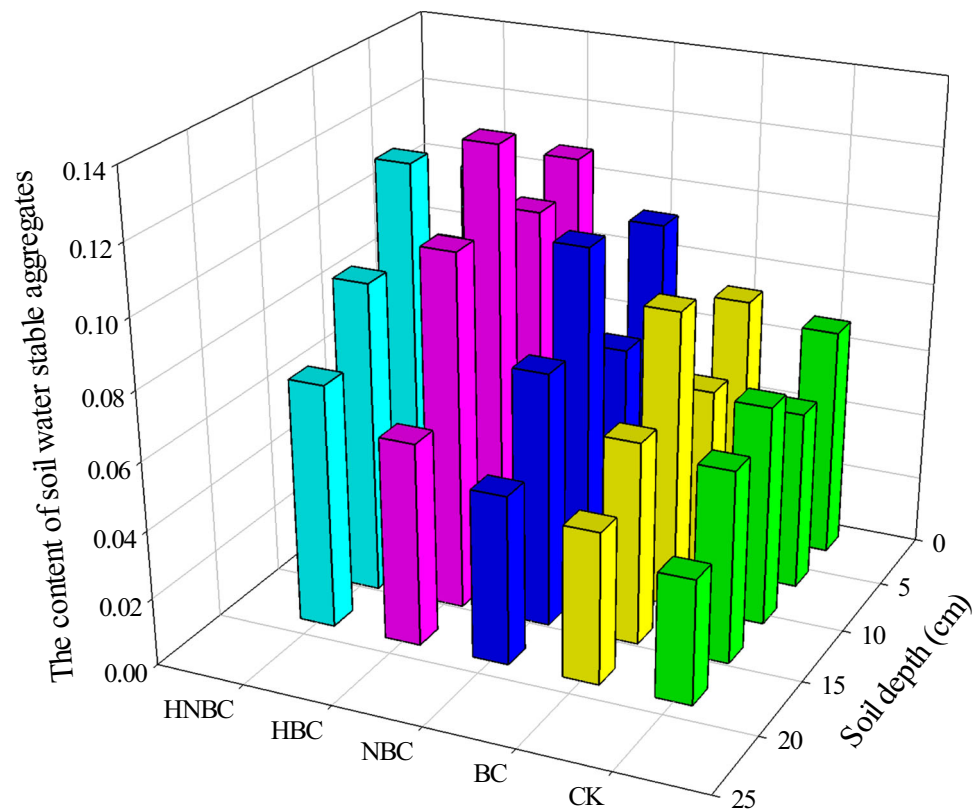




**Table 3** Pearson's correlation coefficients between soil water-stable macro-aggregate contents and soil water contents, salt contents, and soluble Na<sup>+</sup>, K<sup>+</sup>, Ca<sup>2+</sup>, and Mg<sup>2+</sup> contents

	Water content	Salt content	Soil water-stable aggregates	Na <sup>+</sup> content	K <sup>+</sup> content	Ca <sup>2+</sup> content	Mg <sup>2+</sup> content
Water content	1	−0.653**	0.570**	−0.896**	−0.108	−0.359	−0.207
Salt content		1	−0.583**	0.833**	0.079	0.876**	0.580**
Soil water-stable aggregates			1	−0.558**	0.268	−0.351	0.003
Na <sup>+</sup> content				1	0.304	0.556**	0.492*
K <sup>+</sup> content					1	−0.070	0.658**
Ca <sup>2+</sup> content						1	0.606**
Mg <sup>2+</sup> content							1

\*\*  $P < 0.01$ , highly significant correlation; \*  $P < 0.05$ , significant correlation

and effectively reducing the fragmentation of soil macro-aggregates (Joseph et al. 2010; Lu et al. 2014; Dong et al. 2016). Sun et al. (2020) showed that adding biochar to soil significantly increased soil aggregation, but the biochar content inside soil aggregates was low, and thus biochar had an indirect effect on the increased amount of soil aggregates. Zheng et al. (2018) showed that oxidized carboxyl groups and minerals interacted in biochar, where biochar could combine with soil particles and organic-inorganic composites to increase the amount of soil aggregates. Biochar acidification had the greatest effect on the formation of soil water-stable macro-aggregates, possibly because acidification increased the density of carboxyl and oxygen-containing functional groups on the biochar surface (Chang et al. 2019), which facilitated the combination of biochar with soil particles to form soil aggregates.

The Pearson's correlations coefficients between the soil water-stable macro-aggregates and the soil water content, salt content, and water-soluble Na<sup>+</sup>, K<sup>+</sup>, Ca<sup>2+</sup>, and Mg<sup>2+</sup> contents are shown in Table 3. These results demonstrate that the soil water-stable macro-aggregate content was positively correlated with the soil water content ( $P < 0.01$ ) but negatively correlated with the salt content and water-soluble Na<sup>+</sup> content ( $P < 0.01$ ). If the sodium ion concentration is excessively high in the soil, the soil colloids are highly dispersed due to the adsorption of large amounts of sodium ions, thereby causing the soil to swell and the soil aggregates to disintegrate (Callaghan et al. 2014). A lack of soil moisture also significantly reduces the macro-aggregate contents and decreases soil aggregate stability (Zhang et al. 2019). Similarly, improving the formation and stability of the soil aggregates will adversely affect the soil moisture and salinity, which will help to increase the soil porosity and soil moisture permeability (Chaganti and Crohn 2015), reduce the soil salinity, and affect the distributions of soluble salts (Xie et al. 2020). In the present study, the results showed that biochar had a strong adsorption effect which reduced the soluble sodium ion content of the soil and enhanced the soil water-holding capacity and increased the soil water content. This promoted the formation and

stabilization of soil water-stable aggregates (Verheijen et al. 2019). In particular, soil amended with HBC resulted in the greatest reduction in salt content and the greatest increases in water-holding capacity, and this contributed to greater soil water-stable macro-aggregate content in the HBC treatment compared to other treatments.

## 4 Conclusions

The porous structure, SSA, and VMIC of acidified biochar increased, which enhanced the hydrophilicity of saline-alkali soil. Adding acidified biochar resulted in the greatest soil infiltration rate and water-holding capacity and lowest soil the salt content and water-soluble Na<sup>+</sup> content in the soil profile by increasing the soil water content and Na<sup>+</sup> adsorption. In turn, it released more K<sup>+</sup>, Ca<sup>2+</sup>, and Mg<sup>2+</sup> into the soil. The effect of biochar on the soil water-stable macro-aggregates was closely related to the soil moisture and sodium ion contents. Adding acidified biochar greatly promoted the formation of soil water-stable macro-aggregates. Therefore, acidified biochar is a suitable amendment for saline-alkali soil. Future research could explore the effects of acidified biochar on crop growth in saline alkali soil, and the minimum application rate promoted the improvement of low yield fields.

**Supplementary Information** The online version contains supplementary material available at <https://doi.org/10.1007/s11368-021-02913-2>.

**Acknowledgements** We thank Dr. Duncan E. Jackson for language editing.

**Funding** This study was funded by the National Natural Science Foundation of China (41807131, 41977007, and 41830754), China Postdoctoral Science Foundation (2019M653707), Natural Science Foundation of Shaanxi Province of China (2019JQ-537 and 2017JM5107), and Research Project of State Key Laboratory of Eco-hydraulics in Northwest Arid Region of China (2019KJCXTD-4 and QJNY-2019-01).

## Declarations

**Conflicts of interest** The authors declare that there are no conflicts of interest. This manuscript has not been previously published and is not currently in press, under review, or being considered for publication by another journal.

## References

- Ahmad M, Lee SS, Lee SE, Al-Wabel MI, Tsang DCW, Ok YS (2016) Biochar-induced changes in soil properties affected immobilization/mobilization of metals/metalloids in contaminated soils. *J Soils Sediments* 17(3):717–730
- Ahmadi SH, Ghasemi H, Sepaskhah AR (2020) Rice husk biochar influences runoff features, soil loss, and hydrological behavior of a loamy soil in a series of successive simulated rainfall events. *CATENA* 192:104587
- Akhtar SS, Andersen MN, Liu F (2015) Residual effects of biochar on improving growth, physiology and yield of wheat under salt stress. *Agr Water Manage* 158:61–68
- Amini S, Ghadir H, Chen C, Marschner P (2015) Salt-affected soils, reclamation, carbon dynamics, and biochar: a review. *J Soils Sediments* 16(3):939–953
- Amoah-Antwi C, Kwiatkowska-Malina J, Thornton SF, Fenton O, Malina G, Szara E (2020) Restoration of soil quality using biochar and brown coal waste: a review. *Sci Total Environ* 722:137852
- Blok C, Van der Salm C, Hofland-Zijlstra J, Streminska M, Eveleens B, Regelink I, Fryda L, Visser R (2017) Biochar for horticultural rooting media improvement: evaluation of biochar from gasification and slow pyrolysis. *Agronomy* 7(1):6
- Callaghan MV, Cey EE, Bentley LR (2014) Hydraulic conductivity dynamics during salt leaching of a sodic, structured subsoil. *Soil Sci Soc Am J* 78(5):1563–1574
- Chaganti VN, Crohn DM (2015) Evaluating the relative contribution of physiochemical and biological factors in ameliorating a saline-sodic soil amended with composts and biochar and leached with reclaimed water. *Geoderma* 259:45–55
- Chang RH, Sohi SP, Jing FQ, Liu YY, Chen JW (2019) A comparative study on biochar properties and Cd adsorption behavior under effects of ageing processes of leaching, acidification and oxidation. *Environ Pollut* 254:113123
- Dong XL, Guan TY, Li GT, Lin QM, Zhao XR (2016) Long-term effects of biochar amount on the content and composition of organic matter in soil aggregates under field conditions. *J Soils Sediments* 16(5):1481–1497
- Gamage DV, Mapa RB, Dharmakeerthi RS, Biswas A (2016) Effect of rice-husk biochar on selected soil properties in tropical Alfisols. *Soil Res* 54(3):302–310
- Günal E, Erdem H, Çelik İ (2018) Effects of three different biochars amendment on water retention of silty loam and loamy soils. *Agr Water Manage* 208:232–244
- Hammer EC, Forstreuter M, Rillig MC, Kohler J (2015) Biochar increases arbuscular mycorrhizal plant growth enhancement and ameliorates salinity stress. *Appl Soil Ecol* 96:114–121
- Hammes K, Smernik RJ, Skjemstad JO, Herzog A, Vogt UF, Schmidt MW (2006) Synthesis and characterisation of laboratory-charred grass straw (*Oryza sativa*) and chestnut wood (*Castanea sativa*) as reference materials for black carbon quantification. *Org Geochem* 37(11):1629–1633
- Horton RE (1933) The role of infiltration in the hydrologic cycle. *EOS Trans Am Geophys Union* 14(1):446–460
- Huang MY, Zhang ZY, Zhu CL, Zhai YM, Lu PR (2019) Effect of biochar on sweet corn and soil salinity under conjunctive irrigation with brackish water in coastal saline soil. *Sci Hortic* 250:405–413
- Ivushkin K, Bartholomeus H, Bregt AK, Pulatov A, Kempen B, De Sousa L (2019) Global mapping of soil salinity change. *Remote Sens Environ* 231:111260
- Joseph SD, Camps-Arbestain M, Lin Y, Munroe P, Chia CH, Hook J, van Zwieten L, Kimber S, Cowie A, Singh BP, Lehmann J (2010) An investigation into the reactions of biochar in soil. *Soil Res* 48(7):501–515
- Kostiakov AN (1932) On the dynamics of the coefficient of water percolation in soils and the necessity of studying it from a dynamic point of view for the purposes of amelioration. *Trans. 6th Comm. Int Soc Soil Russian* 1:7–21
- Kumari KGID, Moldrup P, Paradelo M, Elsgaard L, de Jonge LW (2016) Soil properties control glyphosate sorption in soils amended with birch wood biochar. *Water Air Soil Pollut* 227(6):174
- Li SL, Shangguan ZP (2018) Positive effects of apple branch biochar on wheat yield only appear at a low application rate, regardless of nitrogen and water conditions. *J Soils Sediments* 18(11):3235–3243
- Li RH, Wang JJ, Zhou BY, Awasthi MK, Ali A, Zhang ZQ, Gaston LA, Lahoria AH, Mahar A (2016) Enhancing phosphate adsorption by Mg/Al layered double hydroxide functionalized biochar with different Mg/Al ratios. *Sci Total Environ* 559:121–129
- Li RH, Zhang YC, Deng HX, Zhang ZQ, Wang JJ, Shaheen SM, Xiao R, Rinklebe J, Xi BD, He XS, Du J (2020) Removing tetracycline and Hg(II) with ball-milled magnetic nanobiochar and its potential on polluted irrigation water reclamation. *J Hazard Mater* 384:121095
- Lu SG, Sun FF, Zong YT (2014) Effect of rice husk biochar and coal fly ash on some physical properties of expansive clayey soil (Vertisol). *CATENA* 114:37–44
- Lu HY, Feng YF, Feng YY, Dong Y, Sun HJ, Xing JC, Shao HB, Xue LH, Yang LZ (2019) Cerium-modified biochar: a recycling biomaterial for regulating phosphorus availability in paddy ecosystem from coastal mudflat reclamation. *Geoderma* 346:43–51
- Luo SS, Wang SJ, Tian L, Li SQ, Li XJ, Shen YF, Tian CJ (2017) Long-term biochar application influences soil microbial community and its potential roles in semiarid farmland. *Appl Soil Ecol* 117:10–15
- Luo SS, Wang SJ, Tian L, Shi SH, Xu SQ, Yang F, Lia XJ, Wang ZC, Tian CJ (2018) Aggregate-related changes in soil microbial communities under different ameliorant applications in saline-sodic soils. *Geoderma* 329:108–117
- Mahdi Z, El Hanandeh A, Yu QJ (2019) Preparation, characterization and application of surface modified biochar from date seed for improved lead, copper, and nickel removal from aqueous solutions. *J Environ Chem Eng* 7(5):103379
- Mahmoud E, El Baroudy A, Ali N, Sleem M (2020) Spectroscopic studies on the phosphorus adsorption in salt-affected soils with or without nano-biochar additions. *Environ Res* 184:109277
- Mao JF, Zhang K, Chen BL (2019) Linking hydrophobicity of biochar to the water repellency and water holding capacity of biochar-amended soil. *Environ Pollut* 253:779–789
- Obia A, Mulder J, Martinsen V, Cornelissen G, Børresen T (2016) In situ effects of biochar on aggregation, water retention and porosity in light-textured tropical soils. *Soil Tillage Res* 155:35–44
- Philip JR (1957) The theory of infiltration: 4. Sorptivity and algebraic infiltration equations. *Soil Sci* 84(3):257–264
- Pongkua W, Dolphen R, Thiravetyan P (2020) Bioremediation of gaseous methyl tert-butyl ether by combination of sulfuric acid modified bagasse activated carbon-bone biochar beads and *Acinetobacter indicus* screened from petroleum contaminated soil. *Chemosphere* 239:124724
- Rizwan M, Lin QM, Chen XJ, Li YY, Li GT, Zhao XR, Tian YF (2020) Synthesis, characterization and application of magnetic and acid modified biochars following alkaline pretreatment of rice and cotton straws. *Sci Total Environ* 714:136532

- Sangani MF, Abrishamkesh S, Owens G (2020) Physicochemical characteristics of biochars can be beneficially manipulated using post-pyrolyzed particle size modification. *Bioresour Technol* 306:123157
- Song BQ, Chen M, Zhao L, Qiu H, Cao XD (2019) Physicochemical property and colloidal stability of micron-and nano-particle biochar derived from a variety of feedstock sources. *Sci Total Environ* 661:685–695
- Sun H, Hockaday WC, Masiello CA, Zygourakis K (2012) Multiple controls on the chemical and physical structure of biochars. *Ind Eng Chem Res* 51(9):3587–3597
- Sun ZC, Zhang ZC, Zhu K, Wang ZM, Zhao XR, Lin QM, Li GT (2020) Biochar altered native soil organic carbon by changing soil aggregate size distribution and native SOC in aggregates based on an 8-year field experiment. *Sci Total Environ* 708:134829
- Tan LS, Ma ZH, Yang KQ, Cui QL, Wang K, Wang TT, Wu GL, Zheng JY (2019) Effect of three artificial aging techniques on physicochemical properties and Pb adsorption capacities of different biochars. *Sci Total Environ* 669:134223
- Usman ARA, Al-Wabel MI, Abdulaziz AH, Mahmoud WA, El-Naggar AH, Ahmad M, Abdulelah AF, Abdulrasoul AO (2016) Conocarpus biochar induces changes in soil nutrient availability and tomato growth under saline irrigation. *Pedosphere* 26(1):27–38
- Verheijen FG, Zhuravel A, Silva FC, Amaro A, Ben-Hur M, Keizer JJ (2019) The influence of biochar particle size and concentration on bulk density and maximum water holding capacity of sandy vs sandy loam soil in a column experiment. *Geoderma* 347:194–202
- Vithanage M, Rajapaksha AU, Zhang M, Thiele-Bruhn S, Lee SS, Ok YS (2015) Acid-activated biochar increased sulfamethazine retention in soils. *Environ Sci Pollution Res* 22(3):2175–2186
- Wang SS, Gao B, Li YC, Mosa A, Zimmerman AR, Ma LQ, Harris WG, Migliaccio KW (2015) Manganese oxide-modified biochars: preparation, characterization, and sorption of arsenate and lead. *Bioresour Technol* 181:13–17
- Wang SY, Ai SY, Nzediegwu C, Kwak JH, Islam S, Li Y, Chang SX (2020) Carboxyl and hydroxyl groups enhance ammonium adsorption capacity of iron (III) chloride and hydrochloric acid modified biochars. *Bioresour Technol* 309:123390
- Xiao L, Yuan GD, Feng LR, Bi DX, Wei J, Shen GH, Liu ZH (2020) Coupled effects of biochar use and farming practice on physical properties of a salt-affected soil with wheat–maize rotation. *J Soils Sediments* 20:3053–3061
- Xie T, Reddy KR, Wang CW, Yargicoglu E, Spokas K (2015) Characteristics and applications of biochar for environmental remediation: a review. *Crit Rev Environ Sci Technol* 45(9):939–969
- Xie WJ, Chen QF, Wu LF, Yang HJ, Xu JK, Zhang YP (2020) Coastal saline soil aggregate formation and salt distribution are affected by straw and nitrogen application: a 4-year field study. *Soil Tillage Res* 198:104535
- Xu RK, Zhao AZ, Yuan JH, Jiang J (2012) pH buffering capacity of acid soils from tropical and subtropical regions of China as influenced by incorporation of crop straw biochars. *J Soils Sediments* 12(4):494–502
- Yang XM, Kang K, Qiu L, Zhao LX, Sun RH (2020) Effects of carbonization conditions on the yield and fixed carbon content of biochar from pruned apple tree branches. *Renew Energy* 146(2):1691–1699
- Yue Y, Guo WN, Lin QM, Li GT, Zhao XR (2016) Improving salt leaching in a simulated saline soil column by three biochars derived from rice straw (*Oryza sativa* L.), sunflower straw (*Helianthus annuus*), and cow manure. *J Soil Water Conserv* 71(6):467–475
- Zhang QY, Shao MG, Jia XX, Wei XR (2019) Changes in soil physical and chemical properties after short drought stress in semi-humid forests. *Geoderma* 338:170–177
- Zhao L, Nan HY, Kan Y, Xu XY, Qiu H, Cao XD (2019) Infiltration behavior of heavy metals in runoff through soil amended with biochar as bulking agent. *Environ Pollut* 254:113114
- Zheng H, Wang X, Luo XX, Wang ZY, Xing BS (2018) Biochar-induced negative carbon mineralization priming effects in a coastal wetland soil: roles of soil aggregation and microbial modulation. *Sci Total Environ* 610:951–960
- Zheng H, Wang X, Chen L, Wang ZY, Xia Y, Zhang YP, Wang HF, Luo XX, Xing BS (2018a) Enhanced growth of halophyte plants in biochar-amended coastal soil: roles of nutrient availability and rhizosphere microbial modulation. *Plant Cell Environ* 41(3):517–532
- Zhu Y, Li H, Zhang GX, Meng FJ, Li LF, Wu S (2018) Removal of hexavalent chromium from aqueous solution by different surface-modified biochars: acid washing, nanoscale zero-valent iron and ferric iron loading. *Bioresour Technol* 261:142–150
- Zong YT, Xiao Q, Lu SG (2015) Acidity, water retention, and mechanical physical quality of a strongly acidic Ultisol amended with biochars derived from different feedstocks. *J Soils Sediments* 16(1):177–190

**Publisher's note** Springer Nature remains neutral with regard to jurisdictional claims in published maps and institutional affiliations.